

G. J. Boer

A study of atmosphere-ocean predictability on long time scales

Received: 24 September 1998 / Accepted: 8 October 1999

Abstract Two different methods, one diagnostic and the other prognostic, are used to investigate the predictability of the coupled atmosphere-ocean system on time scales of months to decades. The diagnostic approach analyzes the output of a 200 year coupled model simulation for evidence that the long time scale variability of annual, pentadal, and decadal means of surface air temperature are “potentially predictable”. The prognostic “perfect model” approach analyzes predictability of the system by calculating the rate of separation of a small set of coupled model simulations in terms of monthly and annual means of surface air temperature over the globe. Both approaches give reasonably coherent results. At the shorter of the time scales considered, there is little predictability over land but some evidence of predictability over the tropical Pacific, the Southern Ocean and to some extent the extratropical northern Pacific. At longer time scales there is some slight evidence of predictability over certain land areas and more definite evidence of predictability in the tropical Pacific and Southern Ocean. A new area of predictability emerges in the tropical Atlantic. There are plausible physical mechanisms which may explain these long time scale areas of predictability. Both approaches have the potential of shedding light on the long time scale predictability of the coupled system in more extensive predictability studies of this kind.

1 Introduction

The CLIVAR science plan calls for study of the predictability of the coupled system at time scales from seasonal to decadal and centennial. In the classical definition, “predictability” is an attribute of the physical

system which measures the short-time scale rate of separation of initially close states in a deterministic system. If the difference in these states is identified with error in the initial conditions of a perfect forecast model, then the rate of separation from the true evolution is a measure of the inherent error growth in the system. The classical result is, ideally, an average over many initial conditions and appropriate error distributions. At CLIVAR time scales, classical predictability approaches must be extended to questions of the predictability of the statistics of the system.

A looser definition of “predictability” might characterize predictability studies into; (1) perfect model, (2) practical, (3) analog, and (4) potential predictability studies. Perfect model and practical predictability approaches are prognostic in the sense that they involve the use of numerical and/or statistical models to make forecasts in the presence of initial condition and/or model error. The resulting error growth in perfect or imperfect models gives information on predictability in this sense.

Analog and potential predictability approaches are diagnostic in the sense that observations from the system are analyzed in order to characterize its predictability. In the analog approach, the separation rate of observed states which are initially “close” is studied where the initial differences are viewed as errors in initial conditions.

Potential predictability is a rather more statistical and indirect concept where the argument is that the observed or modelled variability of some mean quantity is greater than can be accounted for by sampling error given the noise in the system. The inference is that this part of the variability arises from physical processes that are, at least potentially, predictable.

Some preliminary aspects of the predictability of the coupled climate system at CLIVAR time scales using results from the CCCma coupled GCM are discussed here. Two of the four predictability approaches are used namely the “potential predictability” and “perfect model” approaches. The practical predictability approach is out of reach at long time scales because of the

G. J. Boer
Canadian Centre for Climate Modelling and Analysis,
Atmospheric Environment Service,
University of Victoria, BC, Canada
E-mail: George.Boer@ec.gc.ca

lack of three-dimensional oceanographic observations to specify initial conditions. The analog approach suffers from a lack of sufficiently close observed initial states in both the real and modelled system.

2 Notation

Basic statistical measures are used in the study. Forecasts (however defined) are denoted as $y(\tau)$ where τ is the forecast range. Corresponding observations are denoted as $x(\tau)$ with the associated climatological value x_0 . A generalized ensemble averaging operation over a number of forecasts is indicated by an overbar $x = \bar{x} + x'$. The error (and anomaly error) is

$$e(\tau) = y(\tau) - x(\tau) = (y - x_0) - (x - x_0) .$$

The systematic error (the error which is common or systematic in the forecasts and so survives the ensemble averaging) and the remaining random error (Boer 1993) are:

$$e = \bar{e} + e' = (\bar{y} - x_0) + (y' - x')$$

and the random error variance can be written as (Boer 1994)

$$\begin{aligned} \overline{e'^2} &= \overline{(y' - x')^2} = (\sigma_y^2(\tau) + \sigma_x^2) \\ &\times \left[1 - \left(\frac{2\sigma_x\sigma_y(\tau)}{\sigma_y^2(\tau) + \sigma_x^2} \right) r_{xy}(\tau) \right] . \end{aligned} \quad (1)$$

Here σ_y and σ_x are the standard deviations of the forecasts and observations and r_{xy} is the correlation between them. Note that $\sigma_y(\tau)$ may be a function of forecast range if the model gains or loses variance during the forecast period.

A scaled error variance of the form

$$f(\tau) = \frac{\overline{e'^2}}{\sigma_y^2 + \sigma_x^2} = 1 - \beta(\tau)r_{xy}(\tau) = 1 - p(\tau) \quad (2)$$

then follows directly. Nominally $f = 0$ at $\tau = 0$ and $f \rightarrow 1$ as $\tau \rightarrow \infty$. The scaled correlation term p , loosely termed the ‘‘predictability’’ here, has the opposite behaviour so that, typically, $p = 1$ at $\tau = 0$ and $p \rightarrow 0$ as $\tau \rightarrow \infty$ as the forecast and observations become decorrelated. Note however, that if the forecast and the observations are anticorrelated at some range, i.e. if $r_{xy} < 0$, then $f > 1$ and $p < 0$ indicating that the forecast has greater error than a climatological forecast.

Finally, a ‘‘cumulative average scaled error’’ and associated ‘‘cumulative scaled predictability’’ is defined as

$$\tilde{f}(\tau) = \frac{1}{\tau} \int_0^\tau f(\tau') d\tau' = 1 - \tilde{p}(\tau) \quad (3)$$

which gives an averaged representation of the error with forecast range. This statistic has the virtue of averaging out the fluctuations of f (and p) which arise by chance agreement and disagreement of the forecast and observations at a point during the forecast period and which might otherwise be interpreted as representing skill. In effect, the statistic represents a measure of ‘‘consistent’’ skill exhibited to the range τ .

While error measures such as these are most commonly applied to instantaneous values of forecast variables in short range numerical weather prediction, they may be equally applied to monthly and seasonal or even annual, pentadal and decadal mean quantities, as is done here.

3 Considerations at longer time scales

The CLIVAR implementation plan (CLIVAR 1997) is currently structured around principal research areas

involving climatological processes and modes of variability (e.g. the monsoon, tropical modes, extra-tropical modes, the thermohaline circulation, and anthropogenic climate change). Latif (1998) reviews interdecadal variability in the coupled system in terms of five main modes or processes. Coupled atmosphere-ocean modes that are discussed include the tropical Pacific ENSO mode, a tropical Atlantic dipole, tropical-midlatitude interactions, and midlatitude gyre modes in both the north Pacific and Atlantic. Latif (1998) also discusses a north Atlantic midlatitude thermohaline mode as primarily an ocean only phenomena. If analysis indicates enhanced predictability in these regions this will suggest possible long-term forecast skill in the coupled system could be associated with these modes.

The existence of long time scales in the coupled system suggests that the system may possess extended predictability but this is not necessarily the case. One possibility is that the ocean simply damps white noise atmospheric forcing and that the long time scale phenomena in the system are a reflection of this process. In that case, no additional dynamical and/or physical processes provide predictive skill at long time scales so this is taken to represent a lower or least-skill limit of predictability.

The ENSO phenomena is a classical example of a coupled atmosphere ocean process which does exhibit predictability. Here both atmosphere and ocean are involved and they feed back physically upon one another to induce behaviour which exhibits both classical and practical predictability. Other coupled processes may also have long time scales but hurdles to practical predictability remain. These include: (1) the robustness of the mechanism, (2) the availability of initial conditions, and, (3) the ‘‘amount’’ of variability involved. If the mechanism being investigated is not robust to modest errors in initial conditions, coupling formulation, model characteristics, or observational error then there is little practical forecasting potential. For the coupled system, the lack of observations in the body of the ocean, together with the problems of model spin-up, means that initializing (and to a lesser extent verifying) the forecast is a major hurdle for practical forecasting. Finally, although mechanisms exhibiting predictability in some statistical sense may exist in the coupled system, their practical importance is small if only a small fraction of the natural variability is involved.

4 Time series aspects

If the long time scale variability of the coupled system is a consequence of the damping of the weather noise forcing in the manner discussed by Hasselman (1976) and Frankignoul and Hasselman (1977), then skillful forecasting is limited by the damping time scale.

In the simplest representation of this idea, the oceanic mixed layer temperature is governed by the simple equation

$$\frac{\partial T}{\partial t} = -\gamma T + \varepsilon \quad (4)$$

where the mixed layer temperature is forced by white (weather) noise ε and is damped about its equilibrium temperature by feedback processes represented by a damping time scale $1/\gamma$. The resulting spectrum of mixed layer temperature is

$$S_T(\omega) = S_\varepsilon/(\omega^2 + \gamma^2)$$

where ω is the frequency. A red spectrum of this kind is often observed for mixed layer temperatures (Manabe and Stouffer 1996). In this case, the long period variations in temperature are due to the damping of the white noise forcing so are unpredictable beyond the time scale this implies. This situation represents a minimum skill level for a forecast.

The first order autoregressive process

$$X_{t+1} = \beta X_t + \varepsilon_t \quad (5)$$

with $\beta = 1 - \gamma\Delta t$ and $|\beta| < 1$ is a discretized version of Eq. (4). For such a process, the resulting statistical relationships are very simple. The variance of X is related to the random forcing ε as

$$\sigma_x^2 = \sigma_\varepsilon^2/(1 - \beta^2) ,$$

a natural decay time scale in units of Δt may be defined as

$$t_d = 1/(1 - |\beta|) ,$$

and the correlation at lag τ is

$$r(\tau) = \overline{X_{t+\tau}X_t}/\sigma_x^2 = \beta^\tau .$$

A ‘‘perfect model’’ forecast equation for the process (5) is

$$Y_{t+1} = \beta Y_t + \varepsilon_t^y$$

where the error ε_t^y has the same statistical properties as ε_t but is uncorrelated with it.

The rate of separation of two states (or the error of a persistence forecast) at forecast range τ is

$$\begin{aligned} \overline{e_p^2}(\tau) &= d^2(\tau) = \overline{(X_{t+\tau} - X_t)^2} = 2\sigma_x^2(1 - r(\tau)) \\ &= 2\sigma_x^2(1 - \beta^\tau) . \end{aligned}$$

The correlation, error variance, and scaled error variance for forecasts are respectively

$$r_{xy}(\tau) = \beta^{2\tau}$$

$$\overline{e^2}(\tau) = \overline{(Y_{t+\tau} - X_{t+\tau})^2} = 2\sigma_x^2(1 - \beta^{2\tau})$$

$$f(\tau) = \frac{\overline{e^2}(\tau)}{2\sigma_x^2} = 1 - r_{xy}(\tau)$$

For a simple damped system like Eq. (4) driven with white noise, these expressions describe the error behaviour and predictive skill.

5 The coupled model

The coupled model used is the CCCma coupled model in which the second generation atmospheric GCM2 (McFarlane et al. 1992; Boer et al. 1992) is coupled to a three dimensional ocean GCM and thermodynamic ice model. The AGCM has T32L10 resolution while the OGCM has twice the horizontal resolution at $1.8^\circ \times 1.8^\circ$ and a vertical resolution of L29. The OGCM is spun-up from rest before coupling and flux adjustment of heat and fresh water flux is employed.

A multi-year control simulation (Flato et al. 2000) and three independent transient climate change simulations (Boer et al. 2000a, b) forced with historical and projected greenhouse gas and aerosol concentrations, nominally from 1900 to 2100, are available.

Diagnostic potential predictability analyses use results from the control simulation. Because of the way the three independent transient climate change simulations are initialized they provide a ‘‘perfect model’’ forecast experiment during the early part of the simulation where greenhouse gas and aerosol forcing is small.

Griffies and Bryan (1997) report on a predictability study of the north Atlantic, following the perfect model approach, and find evidence of predictability on different time scales at different depths and for different variables in this area and Latif and Barnett (1996) investigate the dynamics and predictability in the north Pacific based on a coupled model. The investigation here takes the global view and concentrates on surface air temperature (SAT) as the primary meteorological variable that closely reflects the evolution of the coupled atmosphere/ocean system as well as being of direct practical interest.

6 Potential predictability

Two potential predictability analysis methods are applied to the surface air temperature of the control simulation of the coupled model. In both cases the intent is to show that the null hypothesis of Sect. 4 can be rejected. These are purely diagnostic calculations however and any potential predictability discerned does not necessarily imply that actual predictive skill is available, but rather that the long time scale variability that is observed cannot be accounted for by the simple damping hypothesis of Eq. (4).

6.1 Autoregressive approach

The autoregressive process Eq. (5) representing a simple damped system like Eq. (4) implies a certain limited forecast skill. If, on the other hand, when the data are fit to the autoregressive process the residual ε_t is not simply white noise, then something other than the damping implied by Eq. (4) is operating. This is taken to imply

that there remains part of the variability that is “potentially” predictable.

The challenge is to test if ε_t is white noise in a suitable statistical way. This is done by applying the “portmanteau” test (von Storch and Zwiers 1999) which proceeds by fitting the autoregressive process Eq. (5) to the data and calculating the q -statistic of order k ,

$$q(k) = (N - 1) \sum_{\tau=1}^k r_{\varepsilon\varepsilon}^2(\tau)$$

based on the autocorrelation of the residual ε_t at various lags.

The test is applied to annual means of the control simulation surface air temperature at grid-points over the globe. In order to remove any residual trends in the control run data, which would be interpreted as potential predictability, the data is first linearly detrended in time. The results of this potential predictability analysis of annual mean SAT are shown in Fig. 1a. Shaded areas indicate where the null hypothesis is rejected at the 10, 5 and 1% probability levels and hence where it is judged that there is “potential predictability” in this sense.

6.2 Analysis of variance approach

This approach is used for pentadal and decadal means where the annual averages that enter the pentadal and decadal means are available to estimate noise variance. The statistical idea is that the variable $X_{\alpha\beta}$ is written as

$$X_{\alpha\beta} = \mu + s_{\alpha} + \varepsilon_{\alpha\beta}$$

where α identifies the particular pentade or decade and β the years within that pentade or decade. $X_{\alpha\beta}$ is represented as the sum of the grand mean μ , some potentially predictable source of variability s_{α} that affects the pentadal or decadal means, and the remaining “noise” term $\varepsilon_{\alpha\beta}$ which depends on shorter time scales. Nominally the variance of the pentadal or decadal mean \bar{X}_{α} is $\sigma_{\bar{X}}^2 = \sigma_s^2 + \sigma_{\varepsilon}^2$ and if an estimate of the ratio $\sigma_s^2/\sigma_{\varepsilon}^2 = 1 + \sigma_s^2/\sigma_{\varepsilon}^2$ is sufficiently larger than 1 the conclusion is that $\sigma_s^2 \neq 0$ at some level of statistical confidence. In other words, there is a source of variability of the mean that is not accounted for as the effect of the noise.

The difficulty here is to estimate the noise and this is done following the approach of Zwiers (1996) where an estimate of the short time scale noise is obtained from the component means that enter an average over a longer period. Here the annual means that enter the pentadal or decadal means are used. The test statistic is the F -ratio with $(N - 1, (m - 1)N)$ degrees of freedom calculated as

$$F = \frac{\sum_{\alpha=1}^N (\bar{X}_{\alpha} - \bar{\bar{X}})^2 / (N - 1)}{\hat{\sigma}_{\varepsilon}^2} \quad \text{where}$$

$$\hat{\sigma}_{\varepsilon}^2 = \frac{1}{m} \left[\frac{1}{N(m - 1)} \sum_{\alpha=1}^N \sum_{\beta=1}^m (X_{\alpha\beta} - \bar{X}_{\alpha})^2 \right].$$

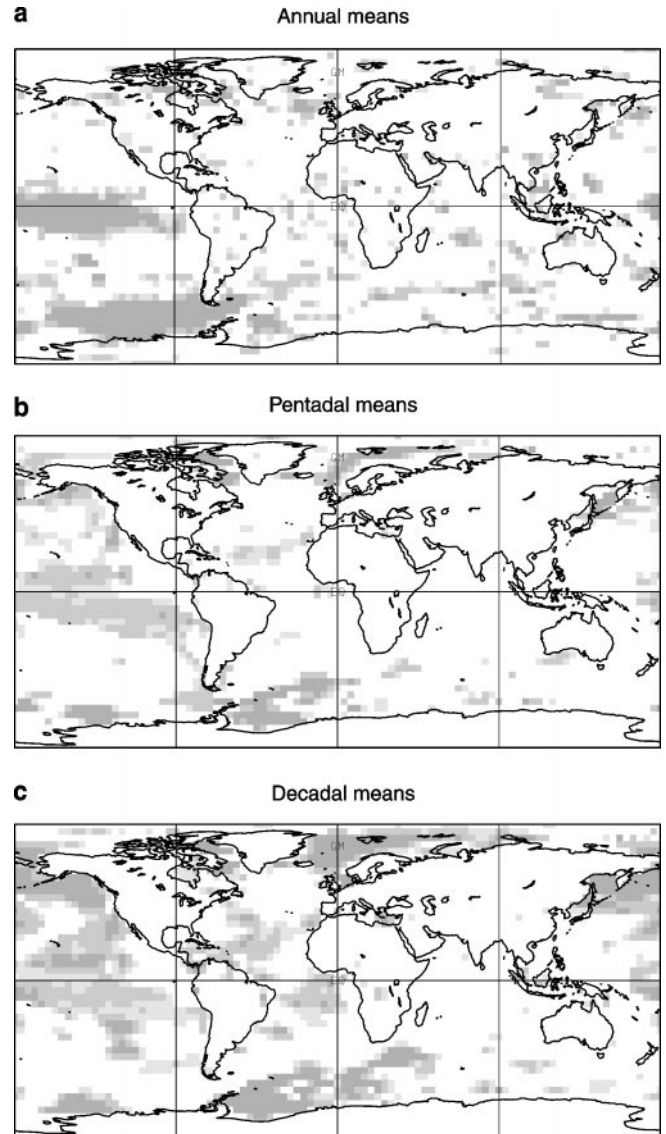


Fig. 1a–c Measures of the potential predictability of **a** annual mean, **b** pentadal mean, and **c** decadal mean surface air temperature in the coupled model. Shading at 10%, 5%, and 1% significance levels. The percentages of the area of the globe shaded at the 5% level are 15%, 11%, and 19% respectively

The data is detrended before the statistical calculation is performed.

This approach assumes that the part of the serial correlation of the annual means within pentades or decades that is associated with the noise is small and so has little effect on the estimate of the noise variance $\hat{\sigma}_{\varepsilon}^2$. The serial correlation of weather noise does not have an appreciable effect on the variability of individual annual means since only a few days at the boundaries of the years are appreciably correlated. Results for potential predictability of pentadal and decadal means are presented in Fig. 1b, c where shaded areas again indicate the 10, 5 and 1% significance levels.

6.3 Long-time scale potential predictability in the coupled system

For *annual mean surface air temperatures*, as shown in Fig. 1a: (1) there is, at best, spotty evidence of potential predictability of the annual mean surface air temperature over the continents; (2) potential predictability in the ENSO region is clearly indicated; (3) a second broad region of potential predictability is indicated in the southern ocean; and (4) there is a suggestion of an area of potential predictability in the north Atlantic.

For *pentadal mean surface air temperatures*, as shown in Fig. 1b: (1) there is even less suggestion of potential predictability over the continents; (2) there is evidence of potential predictability of pentadal means in the ENSO region indicating that the longer time scale variability of this process may be predictable; (3) there is some extension of this apparent area of potential predictability into extra-tropical latitudes in the north Pacific; (4) there is some evidence of an area of potential predictability in the tropical Atlantic; and (5) the strong region of potential predictability in the southern ocean, seen for the annual means, has largely disappeared at this time scale.

For *decadal mean surface air temperatures*, as shown in Fig. 1c: (1) rather extensive regions of potential predictability are apparent including regions in the tropical Pacific and extending into middle latitudes and particularly at high middle latitudes; (2) some tropical Atlantic potential predictability becomes apparent at these time scales; and (3) high latitude potential predictability is apparent in the Atlantic in both hemispheres.

While the connection of these areas of potential predictability with the mechanisms and modes discussed by Latif (1998) is not direct, the connection to ENSO is particularly prominent at the various time scales while the potential predictability of tropical Atlantic and extra-tropical surface air temperatures appears most prominently in decadal means.

The potential predictability over the oceanic areas of the globe suggests the possibility of some long time scale predictability in the system. The oceanic result is certainly not matched by similar areas of potential predictability over land. Over land, the natural variability is larger than over the ocean and whatever predictable mechanisms that exist in the coupled system over the ocean apparently do not propagate their effects to the land areas with a strong enough signal to avoid being swamped by the natural variability in this analysis. This points out once again just how delicate long-term prediction of SAT over land might be expected to be.

7 Perfect model predictability in the coupled system

The “perfect model” approach to predictability has a long history in weather forecasting but has not yet been much used for long time scale studies of predictability in

the global coupled system. A first and rather restricted attempt is presented here. The characteristics of the calculation are as follows:

1. The results are based on three independent simulations of the global coupled model with greenhouse gas and aerosol forcing appropriate to the turn of the century;
2. The simulations are initialized with the *same* three-dimensional oceanic state but with independent 1 January atmospheric states consistent with the forcing;
3. The analysis is confined (at present) to surface air temperature and the “rate of separation” of solutions is taken to give an indication of the error growth rate for the system.

In any real forecast of the coupled system the initial ocean state would also contain error so the predictability investigated here is idealized also in this sense. The longer time scales of the ocean and the rapid growth of error in the atmosphere gives some justification for this approach when investigating the predictability of SAT.

The rate of separation between the i th and j th simulation for the forecast variable y as a function of the range τ is measured by the squared difference in the usual way as

$$d_{ij}^2(\tau) = (y_i(\tau) - y_j(\tau))^2,$$

and the ensemble “separation variance” $\overline{d^2}$, obtained by averaging the d_{ij}^2 over all simulation pairs, is treated as if it were an error variance as discussed in Sect. 2. Here the $y(\tau)$ are *monthly* or *annual* means of SAT.

Because the natural variability of SAT varies greatly over the globe, a plot of $\overline{d^2}$ would have large values in extratropical and smaller values in more tropical regions. The smaller values in the tropics would not imply predictive skill however since the variability there is also low. The scaled quantity

$$f(\tau) = \overline{d^2}/2\sigma^2 = 1 - p(\tau), \quad (6)$$

where σ^2 is the variance obtained from the control run, takes this into account and gives a suitable representation of the “predictability” p which is simply the correlation coefficient in the perfect model case. For presentation purposes, the cumulative scaled predictability $\tilde{p} = 1 - \tilde{f}$ obtained from Eq. (6) is generally used.

7.1 Predictability of monthly mean SAT

Figure 2a shows the cumulative predictability \tilde{p} , calculated for monthly mean SAT, and averaged over the globe, the open ocean, and the land plus sea-ice. Figure 2b shows the corresponding fraction of the area of the globe, open ocean, and land plus sea-ice which displays a level of predictability for which $\tilde{p} > 0.4$. The value for land/ice is comparatively small for the first

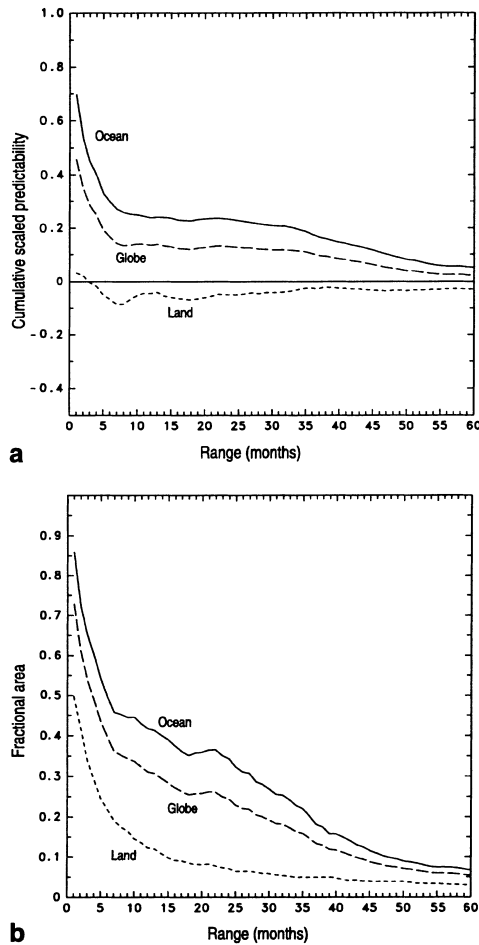


Fig. 2a, b The average of **a** the cumulative predictability \bar{p} of monthly means of surface air temperature over the globe, the open ocean and the land plus sea-ice, and **b** the fraction of the area of these regions which exhibit predictability as measured by $\bar{p} > 0.4$

month and drops rapidly thereafter and this indicates once again the general lack of extended predictability over land and sea-ice.

Over the open ocean, however, the separation of the solutions is considerably less rapid and \bar{p} , and the corresponding fractional area, decrease more slowly indicating possible predictive skill at these time scales. Necessarily, global measures fall between the open ocean and land plus sea-ice values. The message is of a rapid loss of predictability over land and sea-ice and a somewhat slower decrease over the oceans.

The lack of initial predictability over land/ice is consistent with the nature of the initialization of the experiments and the large values of variability found in SAT over land and sea-ice. The values of σ^2 that appear in the denominator of Eq. (6) are the climatological values of the variances of monthly mean SAT calculated separately for each month of the year from the control simulation. The simple average of these twelve monthly values is displayed in Fig. 3 which shows the large values of SAT variance over land and sea-ice.

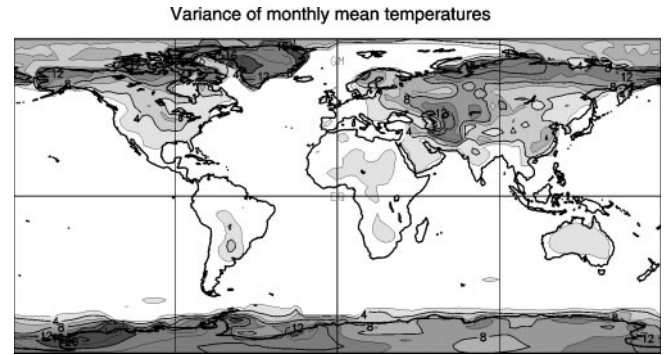


Fig. 3 The simple average of the variances of the monthly mean surface air temperature for each month. These variances are calculated from the 200 year control simulation of the coupled model

If geographically localized coupled modes of the system are predictable, this should be seen in geographically localized regions of higher values of \bar{p} which contrast with regions where the basic damping mechanism Eq. (4) operates and where \bar{p} decreases rapidly. Figure 4 shows the geographical distribution of \bar{p} for monthly mean SAT. Areas with $\bar{p} > 0.4, 0.6$, and 0.8 are shaded. At early times, predictability is seen to fall off rapidly over land and over portions of the oceans at middle latitudes and in some tropical regions. At three months, predictability is concentrated in: (1) the tropical Pacific, (2) the extratropical northern Pacific, (3) the Southern Ocean and (4) certain regions of the north and south Atlantic. By six months, shrunken regions of predictability remain primarily in the first three of these areas.

At even longer times, Fig. 5 shows coherent areas of modest values of \bar{p} fading from the El Niño region of the equatorial Pacific and the near-equatorial Atlantic while remaining in the southern Pacific.

7.2 Predictability of annual mean SAT

Figures 6, 7 and 8 are similar to figures in Sect. 7.1 but now for the *annual mean* SAT. For annual mean SAT, the average of \bar{p} over land plus sea-ice is near zero even for the first annual mean but then increases before decreasing again indicating that, at these longer time scales, there may be some predictability over land induced by that over the oceans. Average \bar{p} over the open ocean is already quite small at year 1 in Fig. 6a and decreases subsequently to year 5, recovers slightly and declines slowly thereafter. The corresponding fractional areas with $\bar{p} > 0.4$ in Fig. 6b show comparatively small differences at the initial period and all decrease more or less uniformly thereafter.

Local values of \bar{p} for annual mean temperatures in Fig. 7 show patterns reminiscent of those for monthly mean temperatures in a broad sense but with some interesting differences. By year 3 there is a general decline in \bar{p} except for: (1) the tropical Pacific region implying

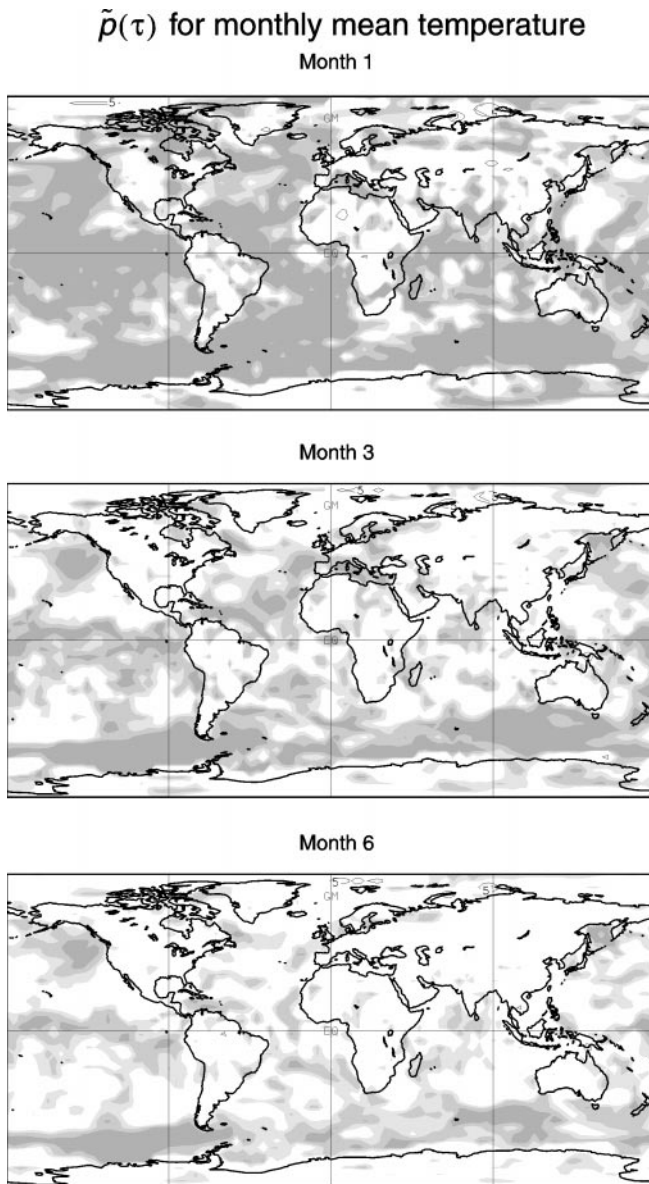


Fig. 4 The geographical distributions of $\tilde{\rho}$ for monthly means of surface air temperature at ranges of 1, 3 and 6 months. Shading boundaries are at $\tilde{\rho} = 0.4, 0.6, \text{ and } 0.8$

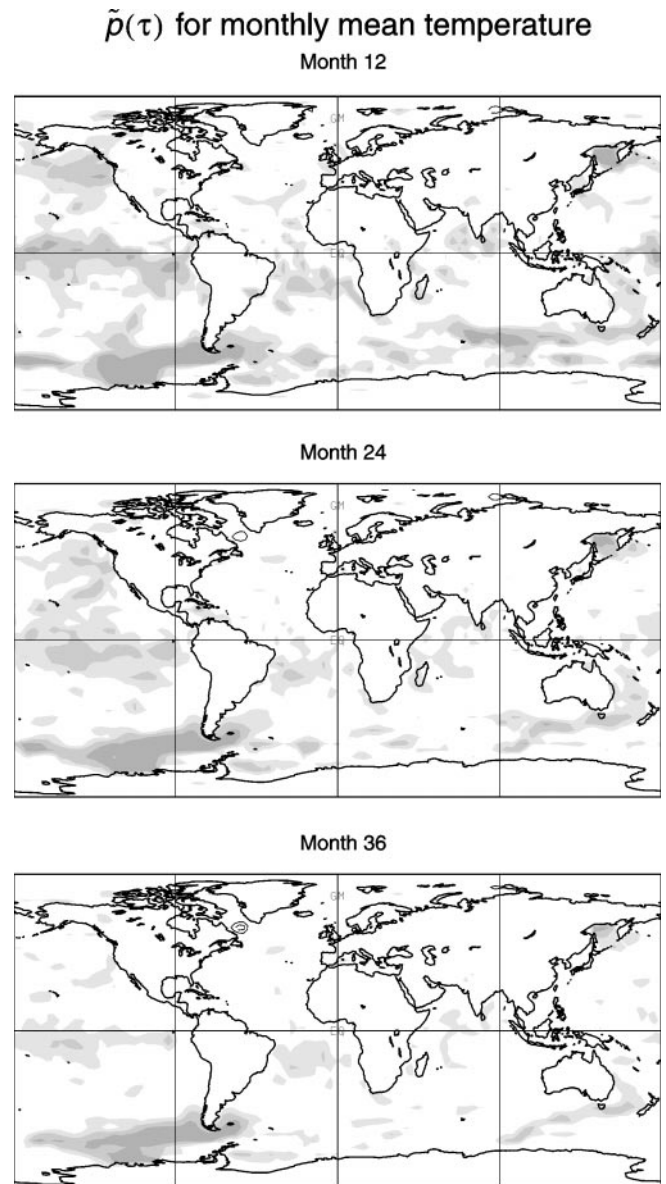


Fig. 5 The geographical distributions of $\tilde{\rho}$ for monthly means of surface air temperature at ranges of 12, 24 and 36 months. Shading boundaries are at $\tilde{\rho} = 0.4, 0.6, \text{ and } 0.8$

predictability associated with the long term variation in ENSO, (2) very modest predictability in the northern Pacific, (3) the Southern Ocean and (4) in the tropical Atlantic. Note however that there are modest regions of apparent predictability over the land for the annual means which were absent for the monthly averages. One implication is that there may be predictable land components of the coupled system on long time scales, due either to local processes or teleconnections with oceanic mechanisms, which are not present (rather which are swamped by short term natural variability) at monthly time scales. The patterns continue to weaken at year 6 and by year 10, most of the predictability is concentrated in the Southern Ocean with some residual shaded values

in the tropical Atlantic and the extratropical northern Pacific. There is, once again, some faint shading over small regions of the northern land area. These patterns continue to weaken at years 20 and 30 with remnants of predictability found only in the Southern Ocean near South America.

8 Discussion

The coupled atmosphere-ocean-land-ice system is expected to exhibit coupled predictability for a richer range of time scales than for the atmosphere alone, which has been the focus of most predictability studies.

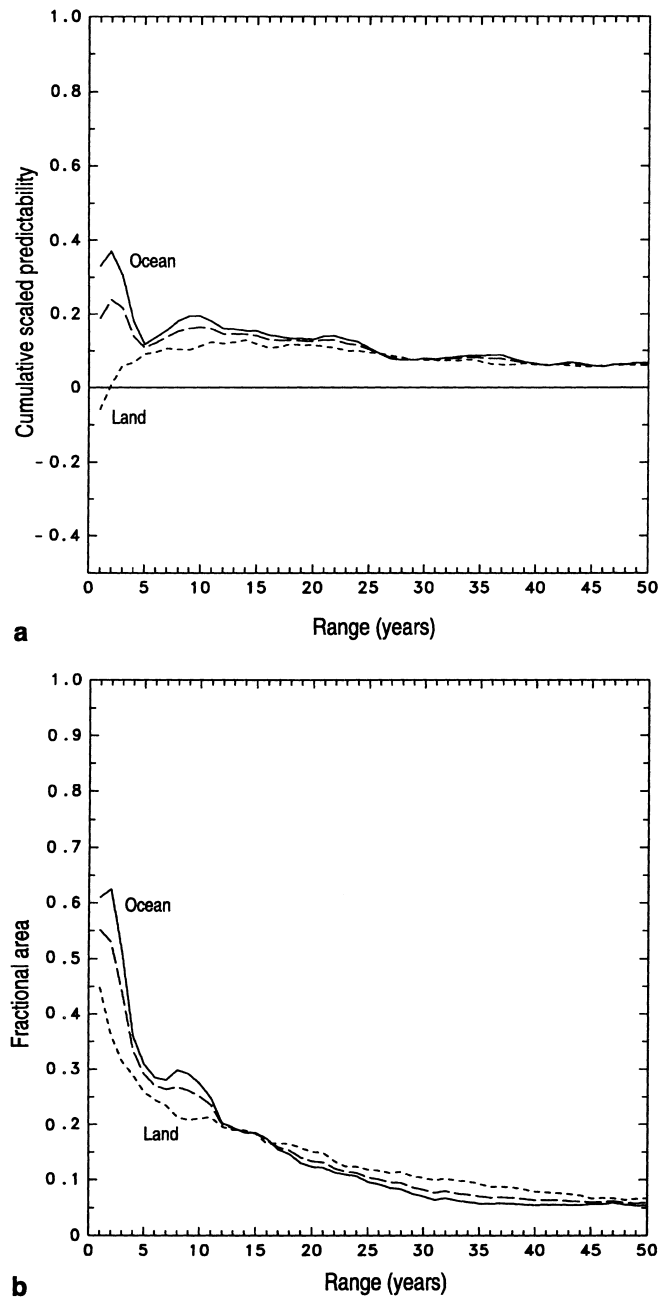


Fig. 6a,b The average of **a** the cumulative predictability of annual means of surface air temperatures over the globe, the open ocean and the land plus sea-ice, and **b** the fraction of the area of these regions which exhibit predictability as measured by $\bar{p} > 0.4$

The CCCma coupled model is used to investigate the long time scale predictability of surface air temperature in the coupled atmosphere/ocean/ice system using both diagnostic “potential predictability” and a prognostic “perfect model” approach. Both approaches give evidence for long time scale predictability in the tropical Pacific, the Southern Ocean and to varying degrees in the tropical Atlantic and the extratropical northern Pacific. Predictability over land and sea-ice is generally weak and, if it exists, appears at longer time scales.

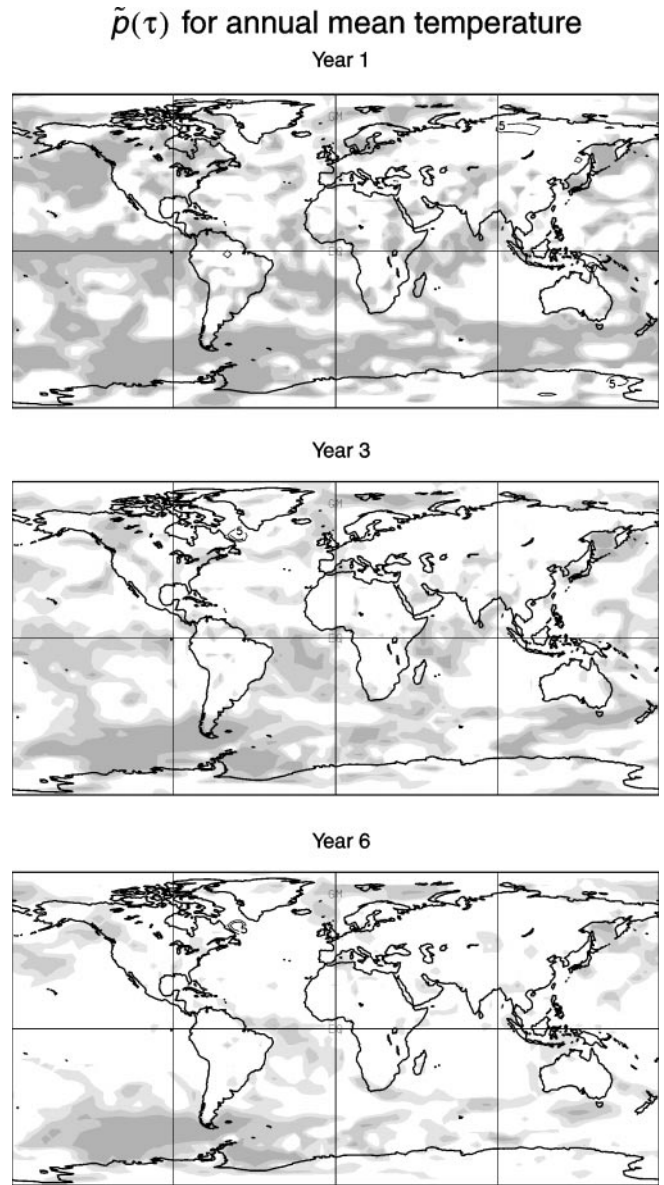
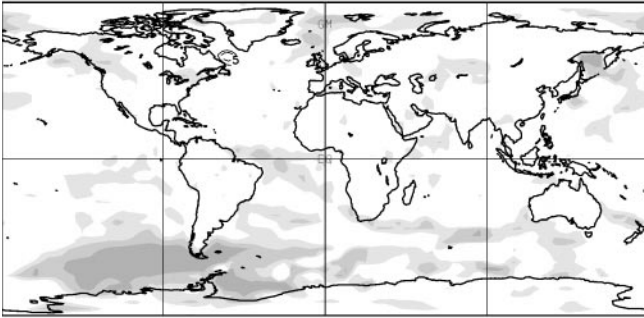


Fig. 7 The geographical distribution of \bar{p} for annual means of surface air temperature at ranges of 1, 3 and 6 years. Shading boundaries are at $\bar{p} = 0.4, 0.6, \text{ and } 0.8$

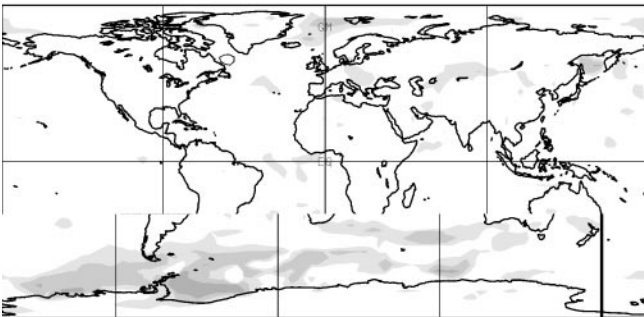
Both predictability approaches have their weaknesses; the potential predictability approach does not directly denote actual predictability, and the perfect model approach may suffer, as its name indirectly implies, from model imperfections as well as from the small number of members in the ensemble. Nevertheless, the results are reasonably complementary and this gives some indication of their robustness. Diagnostic potential predictability studies of simulation results from other models will provide complementary views while a perfect model predictability study with a suite of coupled models and a large ensemble of cases would provide new information on the predictability of the coupled system at long time scales.

$\tilde{\rho}(\tau)$ for annual mean temperature

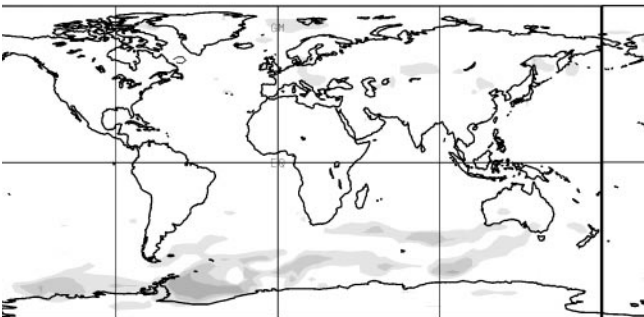
Year 10



Year 20



Year 30



Acknowledgements Greg Flato, Dave Ramsden and Cathy Reader were all involved in the transient simulations from which the data was obtained. Dave Ramsden was particularly helpful in arranging the data in appropriate ways. Francis Zwiers offered statistical advice and he and Greg Flato also provided helpful advice on the manuscript.

References

- Boer GJ, McFarlane N, Lazare M (1992) Greenhouse gas induced climate change simulated with the CCC second-generation general circulation model. *J Clim* 5: 1045–1077
- Boer GJ (1993) Systematic and random error in an extended-range forecasting experiment. *Mon Weather Rev* 121: 173–188
- Boer GJ (1994) Predictability regimes in atmospheric flow. *Mon Weather Rev* 122: 2285–2295
- Boer et al. (2000) A transient climate change simulation with greenhouse gas and aerosol forcing: experimental design and comparison with the instrumental record for the 20th century. *Clim Dyn* 16: 405–425
- Boer et al. (2000) A transient climate change simulation with greenhouse gas and aerosol forcing: projected climate for the 21st century. *Clim Dyn* 16: 427–450
- CLIVAR (1997) Draft implementation plan. Available at <http://www.dkrz.de/clivar/climp.html>
- Flato et al. (2000) The Canadian Centre for Climate Modelling and Analysis global coupled model and its climate. *Clim Dyn* 16: 451–467
- Griffies SM, Bryan K (1997) A predictability study of simulated North Atlantic multidecadal variability. *Clim Dyn* 13: 459–488
- Frankignoul C, Hasselmann K (1977) Stochastic climate models. Part II: application to sea surface temperature variability and thermocline variability. *Tellus* 29: 284–305
- Hasselmann K (1976) Stochastic climate models. Part I: theory. *Tellus* 28: 473–485
- Latif M (1998) Dynamics of interdecadal variability in coupled ocean-atmosphere models. *J Clim* 11: 602–624
- Latif M, Barnett T (1996) Decadal variability over the North Pacific and North America: dynamics and predictability. *J Clim* 9: 2407–2432
- Manabe S, Stouffer RJ (1996) Low-frequency variability of surface air temperature in a 1000-year integration of a coupled atmosphere-ocean-land surface model. *J Clim* 9: 376–393
- McFarlane N, Boer GJ, Blanchet J-P, Lazare M (1992) The Canadian Climate Centre second generation general circulation model and its equilibrium climate. *J Clim* 5: 1013–1044
- Von Storch H, Zwiers F (1999) Statistical analysis in climate research. Cambridge University Press, Cambridge, UK
- Zwiers F (1996) Interannual variability and predictability in an ensemble of AMIP climate simulations conducted with the CCC GCM2. *Clim Dyn* 12: 825–847